Theory of ferromagnetic resonance in magnetic trilayers with a tilted spin polarizer

Peng-Bin He,[1] Zai-Dong Li,[2] An-Lian Pan,[1] Qiang Wan,[1] Qing-Lin Zhang,[1] Ri-Xing Wang,[1] Yan-Guo Wang,[1] Wu-Ming Liu,[3] and Bing-Suo Zou[1]

[1]*Micro-Nano Technologies Research Center, College of Physics and Microelectronics Science, Hunan University, Changsha 410082, China*

[2]*Department of Applied Physics, Hebei University of Technology, Tianjin 300401, China*

[3]*Beijing National Laboratory for Condensed Matter Physics, Institute of Physics, Chinese Academy of Sciences, Beijing 100080, China*

(Received 28 March 2008; revised manuscript received 6 June 2008; published 15 August 2008)

We present a theoretical investigation of ferromagnetic resonance in magnetic trilayers with tilted anisotropy. We find that the resonant magnetic field, the linewidth, the precessional frequency, and the axis of the magnetization in the free layer are all changed by the spin-polarized dc current in the presence of tilted pinned magnetization. Pumping and dissipation of energy in the magnetic system can be controlled by altering the current and the direction of pinned magnetization. The peak of ferromagnetic resonance excited by ac currents is sharpest with pinned magnetization perpendicular to the films, while it is almost flat in the parallel case.

DOI: 10.1103/PhysRevB.78.054420 PACS number(s): 76.50.+g, 72.25.Ba, 75.75.+a

I. INTRODUCTION

The spin-transfer effect proposed by Slonczewski[1] and Berger[2] is of topical interest owing to promising applications in data storage and information processing. In magnetic multilayers, spin-polarized current generated in the pinned layer exerts a spin-transfer torque on the magnetization of the free layer due to the exchange interaction between the conductive electron spin and the local magnetization. Spin-transfer torque provides a new way to drive magnetization switching instead of using a magnetic field.[3,4] Furthermore, it can generate microwave signals[4–6] and influence and even drive ferromagnetic resonance (FMR).[7–14]

FMR is a primary experimental technique for obtaining information on magnetic films,[15] including magnetic anisotropy, magnetic moment,[16] and magnetic damping.[12] Moreover, it can be used to induce magnetization reversal for magnetic particles or an array of interacting particles.[17] Recently, a FMR technique has been developed to detect sub-100-nm-scale devices.[12,13] Spin-transfer-driven FMR measurements have been presented in magnetic multilayers with longitudinal[13] and perpendicular[12,14] anisotropy. The effects of spin-polarized current[7] and interlayer exchange coupling[8] on Gilbert damping have been studied by FMR experiments. Theoretically, spin-current effect on FMR and ac current-driven FMR have been investigated in different magnetic nanostructures.[9–11]

Up to now, attention has been mostly focused on the structures with easy axis parallel or perpendicular to the plane of samples. Magnetic films with tilted anisotropy have been studied by several authors. Shin and Agarwala[18] proposed a method for obtaining tilted magnetic anisotropy in TbFe thin films. Layadi[19] investigated the effects of oblique anisotropy on FMR modes in single and coupled layers. Media with tilted magnetic anisotropy have potential application in high-density magnetic recording.[20] It is also interesting to investigate the magnetic dynamics of multilayers with tilted anisotropy. Except for the direction and magnitude of spin-polarized current, turning the direction of pinned magnetization provides a new choice of controlling the damping and resonant magnetic field. Investigation of FMR in tilted magnetic multilayers is helpful in understanding and controlling magnetic damping. This is important for minimizing the critical current density in current-induced magnetization reversal.

In this paper, we present a study of FMR in magnetic trilayers with a tilted spin polarizer. By a linearization method, the Landau-Lifshitz-Gilbert-Slonczewski equation is reduced to a forced oscillation equation. By using this equation, we investigate the effects of spin-polarized dc current and different directions of pinned magnetization on FMR. The FMR driven by ac current is also discussed.

II. TILTED MAGNETIC TRILAYERS

We consider magnetic trilayers consisting of two ferromagnetic metallic layers with a sandwiched normal metallic spacer. As shown in Fig. 1, the easy axis is along the x direction in the free layer FM_2, while magnetic anisotropy in the pinned layer FM_1 can be altered in different trilayers. Tilted anisotropy may be prepared by oblique incidence evaporation[18] or by applying an oblique magnetic field during the film growth. The polar and azimuth angles of easy axis in the pinned layer are denoted as θ_p and ϕ_p, respectively. With electrical current flowing perpendicularly

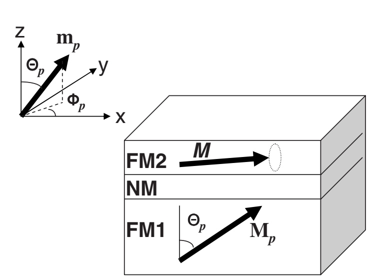

FIG. 1. Schematic drawing of magnetic trilayer with a tilted spin polarizer. The bottom layer FM_1 with pinned magnetization acts as a spin polarizer, The magnetization of the top layer FM_2 is free under magnetic field or current.

through the trilayer, spin polarization takes place in the pinned layer and the magnetization of the free layer undergoes a spin-transfer torque generated by the spin-polarized current. Phenomenologically, the magnetization dynamics of the free layer can be described by the Landau-Lifshitz-Gilbert equation including the spin torque term,[1,21]

$$\frac{d\mathbf{M}}{dt} = \gamma \mathbf{M} \times \frac{\partial E}{\partial \mathbf{M}} + \frac{\alpha}{M_s}\mathbf{M} \times \frac{d\mathbf{M}}{dt} + \frac{\gamma a_J}{M_s}\mathbf{M} \times (\mathbf{M} \times \mathbf{m}_p), \tag{1}$$

where γ is the gyromagnetic ratio, α is the Gilbert damping constant, $\mathbf{M}$ is the magnetization vector of the free layer, M_s is its saturation magnetization, and $\mathbf{m}_p = (\sin\theta_p \cos\phi_p, \sin\theta_p \sin\phi_p, \cos\theta_p)$ is the unit vector of magnetization in the pinned layer. The spin torque parameter a_J is proportional to the current density and dependent on the materials. In general, $a_J = \hbar/(2eM_s d) gJ$, with $g = 1/[-4+(3+\mathbf{M}\cdot\mathbf{m}_p/M_s)(1+P)^3/(4P^{3/2})]$, where d is the thickness of the free layer, P is the spin polarization of the ferromagnet, and current density J takes a positive value when the current flows from the pinned layer to the free one. In our consideration, the energy density consists of anisotropic energy, demagnetization energy, and Zeeman energy, $E = K\sin^2\phi - H_s M_s \sin\theta \cos\phi - H_\perp M_s \sin\theta \sin\phi + 2\pi M_s^2 \cos^2\theta$, where K is the anisotropy constant. Strictly, the anisotropy energy is $K(1-\sin^2\theta\cos^2\phi)$. In view of strong shape anisotropy ($K \ll 2\pi M_s^2$), it is reasonable to assume $E_k = K\sin^2\phi$. In the typical manner of a FMR experiment, the external magnetic fields include a static magnetic field and a rf magnetic field with small amplitude. The static magnetic field $\mathbf{H}_s$ is applied along the x direction, while the rf magnetic field $\mathbf{H}_\perp$ is applied along the y direction.

For convenience, we transform Eq. (1) into a pair of coupled differential equations in polar angle θ and azimuth angle ϕ.[22] Introducing $\psi = \pi/2 - \theta$ and substituting the expression of energy density into Eq. (1), we get

$$\begin{aligned}
-(1+\alpha^2)\frac{d\psi}{dt} = {} & \alpha\gamma \sin\psi (H_s \cos\phi + H_\perp \sin\phi) - \gamma \\
& \times (H_s \sin\phi - H_\perp \cos\phi) \\
& + 2\pi\alpha\gamma M_s \sin 2\psi - \frac{\gamma H_K}{2}\frac{\sin 2\phi}{\cos\psi} \\
& + \gamma a_J \{[-(m_{px}\cos\phi + m_{py}\sin\phi)\sin\psi \\
& + m_{pz}\cos\psi] - \alpha(m_{px}\sin\phi - m_{py}\cos\phi)\},
\end{aligned}$$

$$\begin{aligned}
(1+\alpha^2)\cos\psi \frac{d\phi}{dt} = {} & -\gamma \sin\psi (H_s \cos\phi + H_\perp \sin\phi) \\
& - \alpha\gamma (H_s \sin\phi - H_\perp \cos\phi) \\
& - 2\pi\gamma M_s \sin 2\psi - \frac{\alpha\gamma H_K}{2}\frac{\sin 2\phi}{\cos\psi} \\
& + \gamma a_J \{\alpha[-(m_{px}\cos\phi + m_{py}\sin\phi)\sin\psi \\
& + m_{pz}\cos\psi] + (m_{px}\sin\phi - m_{py}\cos\phi)\},
\end{aligned} \tag{2}$$

where $H_K = 2K/M_s$, representing the anisotropy field. From the energy density, we find that $\theta = \pi/2$ ($\psi = 0$) and $\phi = 0$ at equilibrium without applying current and rf magnetic field. On the basis of Eq. (2), we will discuss FMR driven by rf magnetic fields and spin-polarized ac currents in Secs. III and IV.

III. FERROMAGNETIC RESONANCE EXCITED BY rf MAGNETIC FIELDS

The rf magnetic field is applied usually normal to the static field and expressed as $H_\perp = h_\perp e^{i\omega t}$. Due to the small amplitude of the rf field, the deviation of magnetization from equilibrium position is very small. It is reasonable to take linearization approximation. In the usual FMR experiment of bulk magnet, the trajectory of magnetization forms a cone about the direction of static field. However, in an ultrathin film the very large demagnetization field forces this cone into a very flat ellipse.[22] The motion of magnetization can be reduced to an in-plane rotation and can be described by a one-dimensional equation. After a tedious calculation, a forced oscillation equation about ϕ is obtained from Eq. (2),

$$\frac{d^2\phi}{dt^2} + 2\beta\frac{d\phi}{dt} + \omega_0^2\phi = \omega_0^2\phi_{\text{eq}} + f e^{i\omega t}, \tag{3}$$

where the parameters are given as follows:

$$\beta = \frac{\gamma}{2(1+\alpha^2)}(A' + B' + CD'/A), \tag{4}$$

$$\omega_0 = \frac{\gamma}{1+\alpha^2}(AB + A'B' - C'D' + B'CD'/A)^{1/2}, \tag{5}$$

$$\phi_{\text{eq}} = \frac{\gamma^2(AD' - A'D - CDD'/A)}{(1+\alpha^2)^2\omega_0^2}, \tag{6}$$

$$f = [\gamma(H_s + 4\pi M_s) + i\alpha\omega]\gamma h_\perp/(1+\alpha^2), \tag{7}$$

and

$$A = H_s + 4\pi M_s + \tilde{a}_J[\alpha m_{px} - m_{pz}(m_{py} - \alpha m_{pz})\tilde{g}],$$

$$A' = \alpha(H_s + 4\pi M_s) - \tilde{a}_J[m_{px} + m_{pz}(\alpha m_{py} + m_{pz})\tilde{g}],$$

$$B = H_s + H_K + \tilde{a}_J[\alpha m_{px} - m_{py}(\alpha m_{py} + m_{pz})\tilde{g}],$$

$$B' = \alpha(H_s + H_K) - \tilde{a}_J[m_{px} + m_{py}(m_{py} - \alpha m_{pz})\tilde{g}],$$

$$C = \tilde{a}_J[m_{py} + m_{px}(m_{py} - 3\alpha m_{pz})\tilde{g} + 2m_{pz}^2(m_{py} - \alpha m_{pz})\tilde{g}^2],$$

$$C' = \tilde{a}_J[\alpha m_{py} - m_{px}(\alpha m_{py} - m_{pz})\tilde{g} + 2m_{py}m_{pz}(m_{py} - \alpha m_{pz})\tilde{g}^2],$$

$$D = \tilde{a}_J(m_{py} - \alpha m_{pz}), \quad D' = \tilde{a}_J(\alpha m_{py} + m_{pz}),$$

with $\tilde{a}_J = [2\hbar/(eM_s t)][P^{3/2}/(1+P)^3]\tilde{g}J$ and $\tilde{g} = (1+P)^3/[-16P^{3/2} + (1+P)^3(3+m_{px})]$. Equation (3) describes a forced vibration with damping constant β, precessional angular fre-

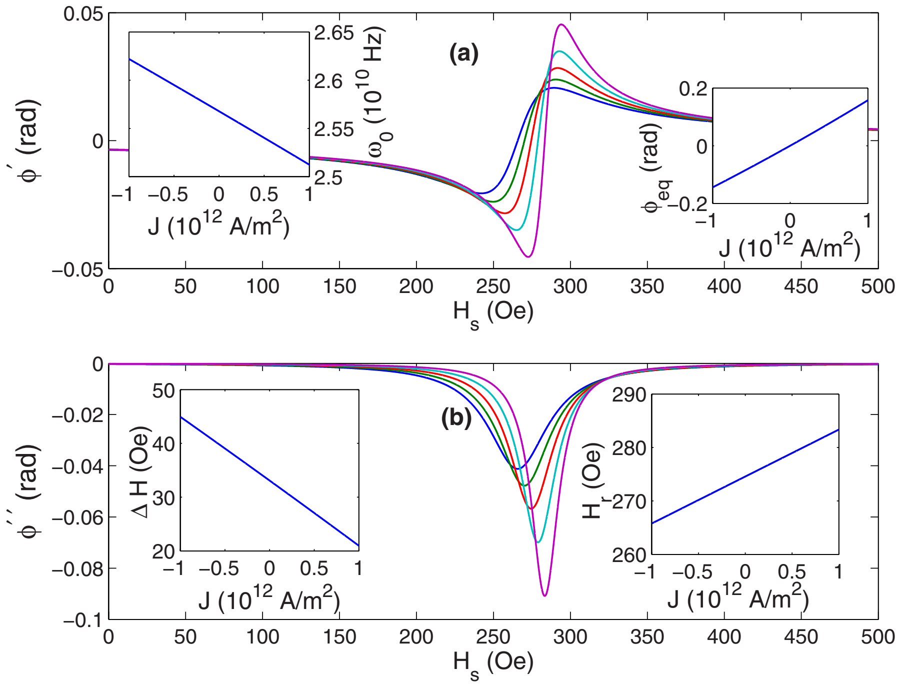

FIG. 2. (Color online) The real (a) and imaginary (b) parts of $\Delta\phi$ as a function of static magnetic field for different currents. The pinned magnetization is along the direction defined by $\theta_p=30°$ and $\phi_p=60°$. The curves from bottom to top correspond to $J=10^{12}$, 5×10^{11}, 0, -5×10^{11}, and -10^{12} A/m^2. The left and right insets of (a) show the dependences of the equilibrium location of ϕ and the precessional angular frequency on current density, respectively. The left and right insets of (b) show the dependence of resonant linewidth ΔH and resonant magnetic field H_r on current density, respectively.

quency ω_0, and driving force f. The amplitude of deviation of ϕ from the equilibrium position is easily obtained,

$$\Delta\phi = \phi' + i\phi'', \tag{8}$$

where the real part ϕ' and the imaginary one ϕ'' have the forms

$$\phi' = \frac{\kappa}{\Lambda}[(\omega_0^2-\omega^2)\gamma(H_s+4\pi M_s)+2\alpha\beta\omega^2],$$

$$\phi'' = \frac{\kappa}{\Lambda}[\alpha\omega(\omega_0^2-\omega^2)-2\beta\omega\gamma(H_s+4\pi M_s)], \tag{9}$$

with $\kappa=\gamma h_\perp/(1+\alpha^2)$ and $\Lambda=(\omega_0^2-\omega^2)^2+4\beta^2\omega^2$.

In the immediate discussion, we take Permalloy as an illustrative instance. The values of related parameters are given as follows: the gyromagnetic ratio $\gamma=1.75\times10^7$ Oe^{-1} s^{-1}, the saturate magnetization $M_s=800$ G, the anisotropic field $H_K=10$ Oe, the Gilbert damping parameter $\alpha=0.01$, the spin polarization $P=0.5$, the thickness of free layer $d=3$ nm, and the frequency of rf magnetic field $\omega=3\times10^{10}$ Hz. The spin torque parameter a_J has the dimension of magnetic field. With the same current density, a_J takes the maximal value in antiparallel configuration, while it takes the minimum in the parallel one. For example, $a_J=178$ Oe with current density 10^{12} A/m^2 and pinned magnetization antiparallel to the free one. Applying the same current, $a_J=25$ Oe in parallel configuration.

Under the dc current, the free magnetization deviates from the original static equilibrium position to a new dynamic one, as shown in the right inset of Fig. 2(a). We will find that in the latter calculation the value of ϕ varies slightly. Along the direction of rf magnetic field, the change in the free magnetization is $\Delta M=M_s[\cos\psi\sin(\phi_{eq}+\Delta\phi)-\cos\psi\sin\phi_{eq}]\approx M_s\Delta\phi$. Therefore, the complex susceptibility is proportional to $\Delta\phi$. In the following, we discuss the FMR properties in terms of $\Delta\phi$.

In FMR experiment, the frequency of rf magnetic field is usually invariable, whereas the static field can be adjusted. In Fig. 2, the resonant curves are shown in different current densities with tilted pinned magnetization. Increasing the current density in the positive direction and decreasing it in the negative direction, the FMR peak turns sharper. From the left inset of Fig. 2(b), we find that in applying positive current (from the pinned layer to the free one), the linewidth becomes narrower and decreases with current density, while in applying positive current the linewidth is broadened and increases with current density. The resonant linewidth is proportional to the effective Gilbert damping parameter. In this case, the positive current pumps energy into the magnetic system, while the negative current dissipates energy away from the system. The left inset of Fig. 2(b) shows that the resonant magnetic field varies with current density in the case of tilted pinned magnetization. Applying dc current, the equilibrium value of ϕ is nonzero, as shown in the right inset of Fig. 2(a). In static state, magnetization precesses around the direction of effective field. The spin-polarized dc current changes this direction, namely, there is a new effective field in the presence of current. Also, the precessional frequency is altered by dc current, as shown in the left inset of Fig. 2(a). The precessional frequency is determined by the static and dynamic torques. The change in frequency is caused by the spin-transfer torque.

Several particular directions of pinned magnetization are picked out to be discussed. For the pinned magnetization parallel to the free one, the resonant magnetic field is determined by $(H_r+4\pi M_s)(H_r+H_K)=\omega^2/\gamma^2-a_J^2$. The maximum of γa_J is on the order of a tenth of ω, so H_r scarcely varies with current density, in agreement with the result in Ref. 9. With pinned magnetization perpendicular to the films, the

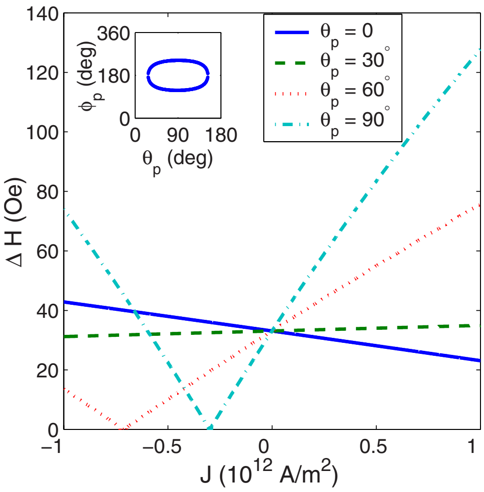

FIG. 3. (Color online) Variation in resonant linewidth ΔH as a function of current density with the directions of pinned magnetization defined by $\theta_p=0,30°,60°,90°$ and $\phi_p=180°$. Inset: In the inner-ellipse region, the linewidth increases with positive current, while in the outer one it decreases with positive current.

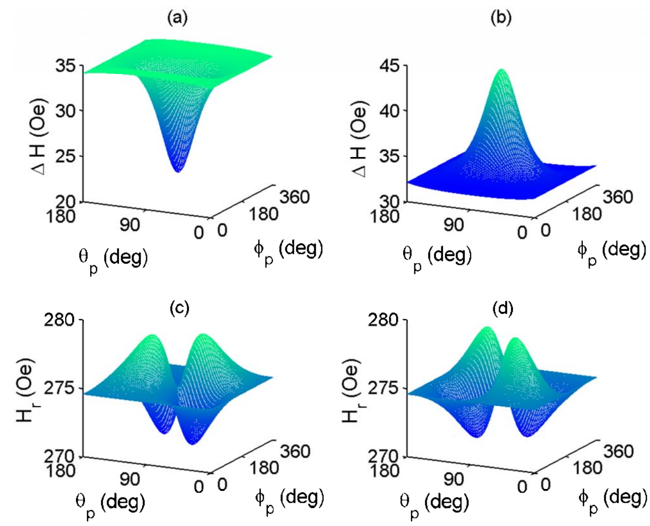

FIG. 4. (Color online) Variation in resonant linewidth ΔH and resonant magnetic field H_r with the direction of pinned magnetization. The current density $J=-10^{11}$ A/m^2 for (a) and (c) 10^{11} A/m^2 for (b) and (d).

resonant field and precessional frequency is unchanged with current. However, the equilibrium location of the free magnetization changes considerably with strong dc current.

Altering the direction of pinned magnetization, the dependence of linewidth on current density is different. Figure 3 shows this dependence in several directions of pinned magnetization with $\phi_p=180°$. For example, in antiparallel configuration energy is dissipated from the magnetic system by positive current, while it is pumped into it by negative current. This is different from the case of $\theta_p=30°$ and $\phi_p=60°$. Especially, the linewidth approaches zero with current density of about -3×10^{11} A/m^2. This means that a very sharp peak appears. In this situation, the energy pumping from current may complement the damping dissipation in the magnetic system. When the orientation of pinned magnetization runs from $\theta_p=28°$ to $\theta_p=152°$ and from $\phi_p=166°$ to $\phi_p=194°$, the linewidth increases with the position current, as shown in the inset of Fig. 3. Outside this region, the linewidth decreases with the position current. In the experiment of Chen *et al.*,[14] the linewidth decreased with the current density and approached zero in a certain value. Though the free layer in this experiment had the perpendicular anisotropy, the dependence of linewidth on current was similar to our results.

We also investigate the dependence of resonant field and linewidth on the direction of pinned magnetization, as shown in Fig. 4. With the pinned magnetization antiparallel to the free one, the resonant linewidth reaches the minimum under negative current, while it reaches the maximum under positive current. By changing the direction of pinned magnetization, we can control the effective damping. With the directions of pinned magnetization defined by $\theta_p=118°$, $\phi_p=148°$ and $\theta_p=62°$, $\phi_p=212°$, the resonant field is highest under negative current. With the directions defined by $\theta_p=62°$, $\phi_p=148°$ and $\theta_p=118°$, $\phi_p=212°$, the resonant field is lowest under negative current. Switching the current direction, the maximal values of resonant field become the minimal ones, and vice versa. Spin current can pump energy into or dissipate energy away from magnets. When the energy gain exceeds the dissipation (including the intrinsic damping), the precession of magnetization can be kept and the switching possibly takes place. The more energy is pumped from current into magnets, the lower threshold current density is needed for switching. It is possible to improve the efficiency of spin-current-related energy pumping by changing the direction of pinned magnetization. We also take Fig. 4 as an example. For the case of $J=-10^{11}$ A/m^2, the pumped energy from current is most with $\theta_p=90°$ and $\phi_p=180°$. For the case of $J=10^{11}$ A/m^2, the pumped energy from current is most in the regions with θ_p between 0 (174°) and 6° (180°) or ϕ_p between 0 (276°) and 84° (360°).

IV. FERROMAGNETIC RESONANCE EXCITED BY SPIN-POLARIZED ac CURRENTS

Instead of the rf magnetic field discussed above, spin-polarized ac current can also excite FMR through ac spin-transfer torque and ac Ampere field. However at sufficiently small size ($\lesssim$100 nm), the spin-transfer effect may dominate. So, we ignore the classical Ampere field in the following. The ac current density takes the form $J=je^{i\omega t}$, with j as the amplitude. Following the same procedure as above, the forced oscillation equation of ϕ is

$$\frac{d^2\phi}{dt^2}+2\beta\frac{d\phi}{dt}+\omega_0^2\phi=f_{ac}e^{i\omega t}, \tag{10}$$

where

$$\beta=\frac{\alpha}{2(1+\alpha^2)}\gamma(2H_s+H_K+4\pi M_s),$$

$$\omega_0=\frac{\gamma}{1+\alpha^2}[(H_s+4\pi M_s)(H_s+H_K)]^{1/2},$$

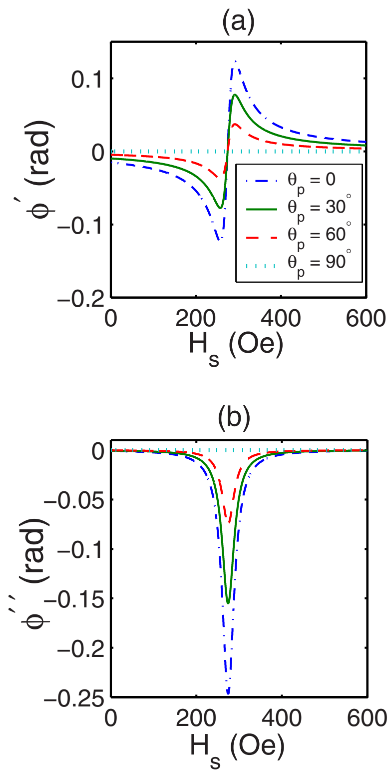

FIG. 5. (Color online) The real and imaginary parts of ϕ as a function of static magnetic field for different directions of pinned magnetization. In both panels, $\phi_p=0$.

$$f_{ac} = \frac{\gamma\tilde{a}_j}{1+\alpha^2}[\gamma(H_s+4\pi M_s)m_{pz} - i\omega(m_{py} - \alpha m_{pz})],$$

with $\tilde{a}_j=2\hbar/(eM_s t)P^{3/2}/[-16P^{3/2}+(1+P)^3(3+m_{px})]j$. By solving Eq. (10), the amplitude of ϕ is obtained,

$$\Phi = \frac{\gamma(H_s+4\pi M_s)m_{pz} - i\omega(m_{py} - \alpha m_{pz})}{\omega_0^2 - \omega^2 + 2i\beta\omega}\gamma\tilde{a}_j. \qquad (11)$$

In Fig. 5, we show the dependence of real part ϕ' and imaginary part ϕ'' of Φ on magnetic field. The frequency of ac current is 3×10^{10} Hz and the amplitude of ac current is 10^{11} A/m^2. In the parallel configuration, no peak emerges. Calculation indicates that to produce an observable peak the current amplitude must be about 10^{16} A/m^2, corresponding to $\tilde{a}_j=2.5\times10^5$ Oe, which is beyond the linear regime. This result is also mentioned in Ref. 9. However, in other tilted configurations, the FMR peak is visible. When the pinned magnetization is perpendicular to the films, the curve is most peaked. The spin-polarized ac current provides an effective rf magnetic field, $a_J/M_s(\mathbf{M}\times\mathbf{m}_p)$. When the pinned magnetization is parallel to the free one, the magnitude of this effective field is very small and not enough to excite a visible resonant peak. On the contrary, the magnitude is maximal in perpendicular configuration. The resonant magnetic field is independent of the direction of pinned magnetization.

V. CONCLUSION

We have investigated the effects of spin-polarized dc current and pinned magnetization on FMR and ac current-driven FMR in tilted magnetic trilayers with linearization method. In the case of rf magnetic-field-excited FMR, the resonant magnetic field, the linewidth, the precessional frequency, and the equilibrium position of free magnetization vary with the dc current density and the direction of pinned magnetization. In the direction of pinned magnetization defined by $\theta_p=90°$ and $\phi_p=180°$, the linewidth reaches extremum. Remarkably, in some directions of pinned magnetization, the linewidth approaches zero with suitable current density. This property can be used to control energy damping in nanomagnets. In the case of ac current-excited FMR, whether the peak emerges is dependent on the direction of pinned magnetization. In the parallel configuration, the required current density for observable resonant peak is beyond the linear regime. In the perpendicular configuration, the peak is sharpest. In this case, the resonant field is irrelative with the direction of pinned magnetization.

ACKNOWLEDGMENTS

This work was supported by NSF of China under Grants No. 10747128 and No. 10647122, Hunan University under Project No. 985, NSF of Hebei Province under Grants No. A2007000006 and No. A2008000006, and Foundation of Education Bureau of Hebei Province under Grant No. 2006110.

[1] J. C. Slonczewski, J. Magn. Magn. Mater. **159**, L1 (1996).
[2] L. Berger, Phys. Rev. B **54**, 9353 (1996).
[3] E. B. Myers, D. C. Ralph, J. A. Katine, R. N. Louie, and R. A. Buhrman, Science **285**, 867 (1999).
[4] G. Bertotti, C. Serpico, I. D. Mayergoyz, A. Magni, M. dAquino, and R. Bonin, Phys. Rev. Lett. **94**, 127206 (2005).
[5] S. I. Kiselev, J. C. Sankey, I. N. Krivorotov, N. C. Emley, R. J. Schoelkopf, R. A. Buhrman, and D. C. Ralph, Nature (London) **425**, 380 (2003).
[6] S. Kaka, M. R. Pufall, W. H. Rippard, T. J. Silva, S. E. Russek, and J. A. Katine, Nature (London) **437**, 389 (2005).
[7] R. Urban, G. Woltersdorf, and B. Heinrich, Phys. Rev. Lett. **87**, 217204 (2001).
[8] K. Lenz, T. Toli nski, J. Lindner, E. Kosubek, and K. Baberschke, Phys. Rev. B **69**, 144422 (2004).
[9] H. Xi, Y. M. Shi, and K. Z. Gao, J. Appl. Phys. **97**, 033904 (2005).
[10] J. N. Kupferschmidt, S. Adam, and P. W. Brouwer, Phys. Rev. B **74**, 134416 (2006).
[11] A. A. Kovalev, G. E. W. Bauer, and A. Brataas, Phys. Rev. B **75**, 014430 (2007).
[12] J. C. Sankey, P. M. Braganca, A. G. F. Garcia, I. N. Krivorotov, R. A. Buhrman, and D. C. Ralph, Phys. Rev. Lett. **96**, 227601 (2006).

[13] G. D. Fuchs, J. C. Sankey, V. S. Pribiag, L. Qian, P. M. Braganca, A. G. F. Garcia, E. M. Ryan, Zhi-Pan Li, O. Ozatay, D. C. Ralph, and R. A. Buhrman, Appl. Phys. Lett. **91**, 062507 (2007).
[14] W. Chen, J.-M. L. Beaujour, G. de Loubens, A. D. Kent, and J. Z. Sun, Appl. Phys. Lett. **92**, 012507 (2008).
[15] M. Farle, Rep. Prog. Phys. **61**, 755 (1998).
[16] Z. Celinski, K. B. Urquhart, and B. Heinrich, J. Magn. Magn. Mater. **166**, 6 (1997).
[17] H. K. Lee and Z. Yuan, J. Appl. Phys. **101**, 033903 (2007); C. Thirion, W. Wernsdorfer, and D. Mailly, Nat. Mater. **2**, 524 (2003).
[18] S. C. Shin and A. K. Agarwala, J. Appl. Phys. **63**, 3645 (1988).
[19] A. Layadi, J. Appl. Phys. **86**, 1625 (1999); Phys. Rev. B **63**, 174410 (2001).
[20] K. Z. Gao and H. N. Bertram, IEEE Trans. Magn. **39**, 704 (2003); Y. Y. Zou, J. P. Wang, C. H. Hee, and T. C. Chong, Appl. Phys. Lett. **82**, 2473 (2003); A. K. Singh, J. Yin, H. Y. Y. Ko, and T. Suzuki, J. Appl. Phys. **99**, 08E704 (2006).
[21] Z. Li and S. Zhang, Phys. Rev. B **68**, 024404 (2003).
[22] D. O. Smith, J. Appl. Phys. **29**, 264 (1958); N. Smith, IEEE Trans. Magn. **27**, 729 (1991); R. F. Soohoo, *Magnetic Thin Films* (Harper & Row, New York, 1965), Chap. 10.